



HAL
open science

Size distributions of elemental carbon in a coastal urban atmosphere in South China: characteristics, evolution processes, and implications for the mixing state

Xiao-Feng Huang, Jian Zhen Yu

► To cite this version:

Xiao-Feng Huang, Jian Zhen Yu. Size distributions of elemental carbon in a coastal urban atmosphere in South China: characteristics, evolution processes, and implications for the mixing state. *Atmospheric Chemistry and Physics Discussions*, 2007, 7 (4), pp.10743-10766. hal-00302999

HAL Id: hal-00302999

<https://hal.science/hal-00302999>

Submitted on 18 Jun 2008

HAL is a multi-disciplinary open access archive for the deposit and dissemination of scientific research documents, whether they are published or not. The documents may come from teaching and research institutions in France or abroad, or from public or private research centers.

L'archive ouverte pluridisciplinaire **HAL**, est destinée au dépôt et à la diffusion de documents scientifiques de niveau recherche, publiés ou non, émanant des établissements d'enseignement et de recherche français ou étrangers, des laboratoires publics ou privés.

Size distributions of elemental carbon in a coastal urban atmosphere in South China: characteristics, evolution processes, and implications for the mixing state

Xiao-Feng Huang and Jian Zhen Yu

Atmospheric, Marine and Coastal Environment Program and Department of Chemistry, Hong Kong University of Science & Technology, Clear Water Bay, Kowloon, Hong Kong, China

Received: 30 May 2007 – Accepted: 19 July 2007 – Published: 25 July 2007

Correspondence to: Jian Zhen Yu (chjianyu@ust.hk)

ACPD

7, 10743–10766, 2007

EC size distributions in an urban atmosphere in China

Xiao-Feng Huang and
Jian Zhen Yu

Title Page

Abstract

Introduction

Conclusions

References

Tables

Figures

⏪

⏩

◀

▶

Back

Close

Full Screen / Esc

Printer-friendly Version

Interactive Discussion

Abstract

Elemental carbon (EC), as one of the primary light-absorbing components in the atmosphere, has a significant impact on both regional and global climate. The environmental impacts of EC are strongly dependent on its particle size. Little is known about the size distribution characteristics of EC particles in the ambient environments of China. We here report size distributions of EC in the urban area of Shenzhen in South China. EC consistently exhibited two modes, a fine and a coarse mode. The majority of EC (~80%) in this coastal metropolitan city resided in particles smaller than $3.2\ \mu\text{m}$ in diameter. The fine mode peaked at around either $0.42\ \mu\text{m}$ or $0.75\ \mu\text{m}$. While the mode at $0.42\ \mu\text{m}$ could be ascribed to fresh vehicular emissions in this region, the mode at $0.75\ \mu\text{m}$ had to be a result of particle growth from smaller EC particles. We made a theoretical investigation of the particle growth processes that were responsible for EC particles to grow from $0.42\ \mu\text{m}$ to $0.75\ \mu\text{m}$ in the atmosphere. Our calculations indicate that the EC peak at $0.75\ \mu\text{m}$ could not be produced through either coagulation or H_2SO_4 condensation; both were too slow to lead to significant EC growth. Hygroscopic growth was also calculated to be impossible. Instead, addition of sulfate through in-cloud processing was found to be able to significantly grow EC particles to explain the EC peak at $0.75\ \mu\text{m}$. We also estimated from the EC size distributions the mixing state of EC. In the droplet size, at least 45–60% of EC mass in the summer samples and 68% of EC mass in the winter samples was internally mixed with sulfate as a result of in-cloud processing. Such information on EC needs to be considered in modeling aerosol optical properties in this region. Our results also suggest that the in-cloud processing of primary EC particles could enhance light absorbing capacities through mixing EC and sulfate.

EC size distributions in an urban atmosphere in China

Xiao-Feng Huang and
Jian Zhen Yu

Title Page

Abstract

Introduction

Conclusions

References

Tables

Figures

⏪

⏩

◀

▶

Back

Close

Full Screen / Esc

Printer-friendly Version

Interactive Discussion

1 Introduction

Elemental carbon (EC) is an important component in atmospheric aerosols and usually considered as the only particulate-phase light-absorbing species in the earth's radiation balance (Horvath, 1993; Jacobson, 2001). Current climatic models predict a positive radiative forcing associated with EC (Hansen et al., 2000; Jacobson, 2001). Model simulations by Menon et al. (2002) indicate that EC emissions from China and India may be responsible for the summer increase in droughts in northeast China and flooding in southeast China observed during the last 20 years. The highest EC concentrations are found in urban atmospheres due to widespread use of fossil fuels, such as diesel and gasoline-powered vehicles.

The light absorption efficiency of EC is a function of particle size (Chuang et al., 2003) and mixing state with other aerosol species (Jacobson, 2001; Lesins et al., 2002). The absorbance coefficients of particles of internally mixed EC and sulfate ammonium are much higher than in externally mixed EC and sulfate particles (Haywood and Shine, 1995; Seinfeld and Pandis, 1998). When EC particles are freshly emitted, they are externally mixed, distinct from other airborne species. After emission, various evolution processes in the atmosphere, such as coagulation, vapor condensation, and cloud (/fog) processing, mix EC with other chemical species and consequently grow EC particles. When assuming different EC mixing states in a global climatic model, Jacobson (2000) showed that the positive radiative forcing of internally mixed EC was about three times higher than that from the externally mixed EC because of a larger absorption cross section in the internal mixing case. It is clear that the knowledge of EC size distributions is essential in accurately modeling its role in modulating regional and global climate.

Atmospheric abundance of EC has been measured in bulk aerosols in numerous studies. The concentration of EC in bulk aerosols ranges from 0.2–2.0 $\mu\text{g}/\text{m}^3$ in rural and remote areas to 1.5–20 $\mu\text{g}/\text{m}^3$ in urban areas (Seinfeld and Pandis, 1998). In comparison, measurements of EC size distributions are considerably fewer, especially

EC size distributions in an urban atmosphere in China

Xiao-Feng Huang and
Jian Zhen Yu

Title Page

Abstract

Introduction

Conclusions

References

Tables

Figures

⏪

⏩

◀

▶

Back

Close

Full Screen / Esc

Printer-friendly Version

Interactive Discussion

**EC size distributions
in an urban
atmosphere in China**

Xiao-Feng Huang and
Jian Zhen Yu

[Title Page](#)[Abstract](#)[Introduction](#)[Conclusions](#)[References](#)[Tables](#)[Figures](#)[⏪](#)[⏩](#)[◀](#)[▶](#)[Back](#)[Close](#)[Full Screen / Esc](#)[Printer-friendly Version](#)[Interactive Discussion](#)

in the urban environments of China, including the Pearl River Delta (PRD) region, a fast-developing economic zone located on the southern coast of China. The ambient concentration levels of EC in $PM_{2.5}$ or PM_{10} in the PRD region are reported in a number of studies (e.g. Cao et al., 2004; Yu et al., 2004; Louie et al., 2005; Hagler et al., 2006).

5 Hagler et al. (2006) measured EC in $PM_{2.5}$ in the PRD region in different seasons during 2002–2003. They reported annual mean EC concentrations of 0.8–4.4 $\mu\text{g}/\text{m}^3$ at seven different sites distributed in urban, regional, and rural surroundings. EC was found to be strongly influenced by local sources, with the highest levels in the urban areas.

10 We report here measurements of EC size distributions in Shenzhen (113.9° E, 22.6° N), a mega-city in the PRD region, and compare them with that of primary vehicular emissions recently measured in a roadway tunnel in this region by our group (Huang et al., 2006a). A second objective is to theoretically examine possible atmospheric aerosol evolution processes that could lead to the EC size distributions as
15 observed in Shenzhen. A third objective is to estimate EC mixing state using the size distribution data and to discuss the implications. Such information is needed to model the radiative forcing of EC and hence the role of EC as a modulator of regional and global climate.

2 Aerosol sampling and chemical analysis

20 The sample collection and chemical analysis details have been described in our previous paper (Huang et al., 2006b). A brief account is given below. Size-segregated aerosol samples in the size range of 0.056–18 μm were collected onto quartz fiber filter substrates using a ten-stage microorifice uniform deposit impactor (MOUDI) without rotation. Nine sets of summer samples were collected during July–August 2004, and
25 twelve sets of winter samples were collected from December 2004 to January 2005. Each sampling event lasted 48 or 72 h.

Each filter substrate was analyzed for ionic species (i.e. Cl^- , NO_3^- , SO_4^{2-} , oxalate,

Na⁺, NH₄⁺, K⁺, Mg²⁺, and Ca²⁺), organic carbon (OC) and EC (Huang et al., 2006b). The OC/EC analysis was made on one quarter of each quartz filter using a thermal/optical transmittance aerosol carbon analyzer (Sunset Laboratory, OR) (Birch and Cary, 1996). The temperature program for the thermal analysis was the same as that in the NIOSH method for diesel soot (NIOSH, 1999). The entire analytical cycle is 580 s and 1% O₂ is introduced into the helium carrier gas at 360 s into the analysis. Due to the non-uniform deposition nature of the MOUDI samples, charring correction using optical transmittance could not work properly to set the OC and EC split point (Chow et al., 1993). We first varied the OC/EC split time from 360 s (i.e. no charring correction) to 420 s, the typical split time range found for bulk aerosol samples in this region. Figure 1 is an example of size distribution of EC obtained using three different fixed split time positions (360, 400, and 420 s). As expected, the EC concentrations depend strongly on where the split point was set. The EC concentrations obtained without charring correction could be up to 2 times those obtained with the split time set at 420 s. However, the different split times had little influence on the size distribution pattern. That is, regardless of the OC/EC split position, EC always showed a dominant fine mode in the same size bin (0.32–0.56 μm in this example). As a result, the uncertainty in the EC/OC split point did not affect the discussion below on the evolution of EC size distributions. For lack of a better alternative, the OC/EC split time was fixed at 360 s, i.e. with no charring correction. By our operational definition, OC is the fraction of carbon that evolved at or below 850 °C in a helium atmosphere, and EC is the fraction of carbon that evolved after 1% oxygen is introduced to the carrier gas during an analytical cycle.

3 Results and discussion

3.1 EC size distributions

Table 1 lists the EC concentrations in fine (<3.2 μm in diameter) and coarse particles (>3.2 μm in diameter) in individual samples. The fine mode EC had an average con-

EC size distributions in an urban atmosphere in China

Xiao-Feng Huang and
Jian Zhen Yu

Title Page

Abstract

Introduction

Conclusions

References

Tables

Figures

⏪

⏩

◀

▶

Back

Close

Full Screen / Esc

Printer-friendly Version

Interactive Discussion

centration of $4.5 \mu\text{g}/\text{m}^3$ in the summer samples and $8.1 \mu\text{g}/\text{m}^3$ in the winter samples. The fine mode EC accounted for approximately 80% of the total EC in both the summer and the winter samples. The higher concentrations of EC in winter were a combined result of the unfavorable atmospheric dispersion conditions and little wet removal in winter in the PRD region (Yuan et al., 2006).

The average EC size distributions in the summer and the winter samples are shown and compared with the EC size distribution obtained in a roadway tunnel in this region in Fig. 2. The ambient EC showed a common bimodal pattern, with a major fine mode and a minor coarse mode. While the coarse mode always peaked in the size bin of $3.2\text{--}5.6 \mu\text{m}$, the fine mode peaked in one of the two size bins of $0.32\text{--}0.56 \mu\text{m}$ and $0.56\text{--}1.0 \mu\text{m}$. Among the nine sets of the summer samples, six sets with lower EC concentrations (Group L) peaked in the size bin of $0.32\text{--}0.56 \mu\text{m}$ while the other three sets with higher EC concentrations (Group H) peaked in the size bin of $0.56\text{--}1.0 \mu\text{m}$. The average EC size distributions of Groups L and H were also shown in Fig. 2a. In comparison, all the twelve sets of the winter samples consistently showed a fine mode EC peak in the size bin of $0.56\text{--}1.0 \mu\text{m}$. This is a logic result of frequent wet removal of aged aerosols ($0.56\text{--}1.0 \mu\text{m}$) in the summer, leading to a more prominent presence of freshly emitted EC ($0.32\text{--}0.56 \mu\text{m}$). The rainfall amount in the summer sampling periods was recorded to be 495 mm while there was only 6 mm rainfall in the winter sampling periods.

A fine mode EC peaking in the size bin of $0.32\text{--}0.56 \mu\text{m}$ was consistent with a scenario in which the ambient EC particles were dominated by freshly emitted EC particles from vehicular emissions. Such a scenario could be possibly developed after a heavy rain event removed most of the aged EC particles. The size distribution characteristics of EC particles from vehicular emissions in this region were previously measured in a roadway tunnel by our group and were found to exhibit a dominant fine mode peaking in the size bin of $0.32\text{--}0.56 \mu\text{m}$ (Fig. 2c). The study by Hagler et al. (2006) on the temporal and spatial distribution of major aerosol constituents in $\text{PM}_{2.5}$ presented evidence to indicate that local vehicular exhaust was the dominant source of EC in

EC size distributions in an urban atmosphere in China

Xiao-Feng Huang and
Jian Zhen Yu

Title Page

Abstract

Introduction

Conclusions

References

Tables

Figures

⏪

⏩

◀

▶

Back

Close

Full Screen / Esc

Printer-friendly Version

Interactive Discussion

the urban atmosphere in the PRD region. In comparison with freshly emitted EC from vehicles, apparently on many days, the ambient EC size distribution shifted towards a larger size, which was clearly indicated by the shift of the modal peak from 0.32–0.56 μm to 0.56–1.0 μm in all the winter samples and in three summer samples. This shift must be a result of atmospheric aging of fresh EC after emissions. What is the mechanism responsible for the growth of fresh EC particle to the 0.56–1.0 μm mode in this region? This is an important question because the particle size of EC strongly influences its lifetime and optical properties in the atmosphere. We present below a theoretical investigation aiming to identify the responsible mechanism.

3.2 Theoretical analysis of EC growth mechanisms

To explain the presence of the 0.56–1.0 μm mode is in essence to identify a mechanism by which EC particles of 0.32–0.56 μm grow to 0.56–1.0 μm . In the atmosphere, aerosol particles can grow in size through several mechanisms, including water accretion, coagulation, vapor condensation, and addition of materials formed through heterogeneous or in-cloud (fog) aqueous reactions. To quantify the extent of growth by the various processes, we must consider the number size distributions and thermodynamic properties of the aerosol particles. The number size distributions were estimated from the measured mass size distributions with the following consideration: (1) All particles in each size bin were assumed to have the mean diameter and the same chemical composition; (2) The particle density in each size bin was the mass-weighted average density of the measured constituents, including EC, OC, Cl^- , NO_3^- , SO_4^{2-} , Na^+ , NH_4^+ , K^+ , Mg^{2+} , and Ca^{2+} , and water; (3) Contribution of the aerosol water content was calculated using an aerosol thermodynamic model, ISORROPIA (Nenes et al., 1998) and assuming a relative humidity (RH) of 78%, the mean value during the summer sampling periods; and (4) Crustal materials were not included in the chemical composition on the basis that they usually contribute little to the total mass in fine aerosol particles. Considering that Group L aerosol represented relatively freshly emit-

EC size distributions in an urban atmosphere in China

Xiao-Feng Huang and
Jian Zhen Yu

[Title Page](#)[Abstract](#)[Introduction](#)[Conclusions](#)[References](#)[Tables](#)[Figures](#)[⏪](#)[⏩](#)[◀](#)[▶](#)[Back](#)[Close](#)[Full Screen / Esc](#)[Printer-friendly Version](#)[Interactive Discussion](#)

ted particles, we used the average aerosol size distributions of Group L aerosol to approximate the starting particle population for growth estimation.

The temporal and spatial scales relevant to our discussion are described as below. We define the so-called “local” region to be the entire highly urbanized PRD region of about $2^{\circ} \times 2^{\circ}$ (200 km \times 200 km). Backward trajectories of 100 m above ground were calculated for all the summer sampling days using the hybrid single-particle Lagrangian integrated trajectories (HYSPLIT) model (<http://www.arl.noaa.gov/ready/hysplit4.html>). The back trajectory calculations indicated that air masses resided in the PRD region for about 12–24 h before they were transported outside. We adopted 1 day as the upper limit for the residence time of locally emitted EC in the PRD region.

3.2.1 Hygroscopic growth

When RH increases, hygroscopic components in particles take up water. The amount of water accretion can be calculated using the thermodynamic model ISORRPIA. Figure 3 shows the calculated particle growth as a function of ambient RH from 70 to 95% when a particle of $0.42 \mu\text{m}$ (the mean diameter of the $0.32\text{--}0.56 \mu\text{m}$ size bin) absorbs water. The particle could at most grow to $0.54 \mu\text{m}$ by water accretion when RH was increased to 95%. Such a high RH scarcely occurs on non-precipitation days. This demonstrates that water accretion is not a viable mechanism for the EC particles in the $0.32\text{--}0.56 \mu\text{m}$ range to grow to the next size bin of $0.56\text{--}1.0 \mu\text{m}$.

3.2.2 Coagulation

Collision of particles can result in coagulation of particles and hence particle growth in size. Coagulation of particles in the atmosphere is dominated by Brownian motions (Wexler et al., 1994). Diffusion coagulation between a smaller particle and a larger particle depletes the smaller particle but does not cause significant particle growth while coagulation between particles of similar sizes is effective for particle growth. When two particles of the same size collide, the resulting particle has a mass equivalent diame-

EC size distributions in an urban atmosphere in China

Xiao-Feng Huang and
Jian Zhen Yu

Title Page

Abstract

Introduction

Conclusions

References

Tables

Figures

⏪

⏩

◀

▶

Back

Close

Full Screen / Esc

Printer-friendly Version

Interactive Discussion

ter up to 1.3 times that of the original one (Kerminen and Wexler, 1995). The nature of coagulation dictates that while coagulation is an effective mechanism for transfer of particles from the nuclei mode ($<0.1 \mu\text{m}$) to the accumulation mode, it is a slow process for growth of particles in the accumulation mode size range (Seinfeld and Pandis, 1998).

We estimated the time needed for the $0.32\text{--}0.56 \mu\text{m}$ size bin to grow into the next size bin of $0.56\text{--}1.0 \mu\text{m}$ by coagulation. The number concentration of particles in the $0.32\text{--}0.56 \mu\text{m}$ size bin was $\sim 200 \text{cm}^{-3}$ during our summer sampling period. Assuming the upper value of the coagulation coefficient, K , of $10^{-9} \text{cm}^{-3} \text{s}^{-1}$, we calculated that the time required was at least 8 days to grow particles to the $0.56\text{--}1.0 \mu\text{m}$ size bin. This time scale was apparently too slow to account for the observed EC mode shift.

3.2.3 Vapor condensation

Particle growth by condensation of gaseous species, heterogeneous reactions, and in-cloud processing is all related to addition of new aerosol materials. We first need to identify the new aerosol materials that are primarily responsible for the EC particle growth in our ambient environment. This was achieved by comparing the relative abundance of the major aerosol components to EC in the two size bins ($0.32\text{--}0.56 \mu\text{m}$ and $0.56\text{--}1.0 \mu\text{m}$) in Group H samples (Fig. 4). Only sulfate and ammonium were significantly more abundant in the $0.56\text{--}1.0 \mu\text{m}$ size bin than in the $0.32\text{--}0.56 \mu\text{m}$ size bin. This comparison identified sulfate and ammonium to be the new aerosol materials responsible for the EC particle growth. Ammonium and sulfate in the two size bins had a molar ratio of 1.9 and 2.0, respectively, indicating that sulfate ammonium was their main aerosol phase form. We next considered secondary formation of ammonium sulfate and subsequent addition to the existing EC particles in the size bin of $0.32\text{--}0.56 \mu\text{m}$.

Among the secondary formation pathways of sulfate aerosol, in-cloud aqueous oxidation of SO_2 has been established to be the dominant mechanism, contributing 50–80% of the conversion from SO_2 to sulfate in the troposphere, followed by gas-phase

EC size distributions in an urban atmosphere in China

Xiao-Feng Huang and
Jian Zhen Yu

Title Page

Abstract

Introduction

Conclusions

References

Tables

Figures

⏪

⏩

◀

▶

Back

Close

Full Screen / Esc

Printer-friendly Version

Interactive Discussion

photochemical oxidation of SO₂ (Langner and Rodhe, 1991; McHenry and Dennis, 1994; Seinfeld and Pandis, 1998; Warneck, 1999). Heterogeneous oxidation of SO₂ on the solid particle surface or in the liquid surface layer of particles is insignificant in submicron particles (Saxena and Seigneur, 1987; Meng and Seinfeld, 1994; Liang and Jacobson, 1999; Kerminen et al., 2000). Therefore, heterogeneous reactions are excluded as a possible mechanism responsible for the significant EC growth in Shenzhen.

Of the gas-phase oxidation reactions of SO₂, the reaction with OH radicals is the dominant pathway, especially in urban environments. The rate constant for this reaction at 298 K is $1.2 \times 10^{-12} \text{ molecule}^{-1} \text{ cm}^3 \text{ s}^{-1}$. In our calculation, we assumed a SO₂ concentration of 10 ppb, the mean concentration level in summer in Shenzhen (SZEPCB, 2006). As there is no available measurement of OH radical concentration in this region, we adopted three [OH] values, 0.5, 0.75, and $1 \times 10^7 \text{ molecules cm}^{-3}$, in the typical range of summer time [OH] (i.e. $0.5 \sim 1 \times 10^7 \text{ molecules cm}^{-3}$) (Seinfeld and Pandis, 1998). The gas-phase H₂SO₄ production rate was calculated to be 2%, 3%, and 4% [SO₂]h⁻¹ at the three OH concentrations, respectively. The time for active photochemical reactions was set to be 8 h per summer day, resulting in a total SO₄²⁻ production of 6.3, 9.5, and 13 μg/m³ at the three production rates, respectively.

The newly formed gas-phase H₂SO₄ subsequently condenses on available particle surface. The particle-size dependent condensation flux can be expressed as (Pandis et al., 1993):

$$J_i = 2 \pi D_p D_i (C_{a,i} - C_{e,i}) / (\beta + 1), \quad (1)$$

where D_p is the particle diameter, D_i is the molecular diffusivity of the condensate i , $C_{a,i}$ and $C_{e,i}$ are the ambient concentration and the equilibrium particle surface concentration, respectively. $\beta = 2\lambda/\alpha D_p$, where α is the accommodation coefficient, and λ is the mean free path of air. The α value of H₂SO₄ was assumed to be size-independent and set at 0.12 (Ervens et al., 2003). Equation (1) indicates that the overall transfer rate to particles in a size bin depends on $n(D_p)J_i$, where $n(D_p)$ is the number of par-

EC size distributions in an urban atmosphere in China

Xiao-Feng Huang and
Jian Zhen Yu

Title Page

Abstract

Introduction

Conclusions

References

Tables

Figures

⏪

⏩

◀

▶

Back

Close

Full Screen / Esc

Printer-friendly Version

Interactive Discussion

ticles of diameter D_p . A constant $C_{e,i}$ of H_2SO_4 was also assumed for all particles. The fraction of the condensed H_2SO_4 in each size bin can be calculated from Eq. (1). About 17% of H_2SO_4 was estimated to condense on particles in the 0.32–0.56 μm size bin. We next assumed that the condensed H_2SO_4 were neutralized by sufficient NH_3 to form $(\text{NH}_4)_2\text{SO}_4$, which caused corresponding increase of aerosol water content. The new particle size after addition of $(\text{NH}_4)_2\text{SO}_4$ and water can thus be obtained. Figure 5 shows the new size distribution of EC after sulfate condensation growth. It can be seen that the EC particles originally of a diameter of 0.42 μm grows to 0.51, 0.55 and 0.58 μm in the three scenarios, respectively. The new particle sizes are still much smaller than the mean diameter of the 0.56–1.0 μm size bin (i.e. 0.75 μm). We therefore conclude that condensation of H_2SO_4 produced in the gas-phase was too slow to account for the growth of EC in the 0.32–0.56 μm size bin to the 0.56–1.0 μm size bin.

3.2.4 In-cloud processing

Stratus and stratocumulus are the most two most common low level clouds, which exist at about 0–2 km from the ground, and thus can significantly promote atmospheric aqueous chemistry in the mixing layer (Meng and Seinfeld, 1994; Seinfeld and Pandis, 1998). The average cloud cover in this coastal region in summer is about 70% (<http://www.hko.gov.hk>). Assuming a typical updraft velocity of 0.05 m/s for stratus and stratocumulus clouds (Venkataraman et al., 2001), we calculated that all air mass in the mixing layer (~ 1.2 km in summer, Yuan et al., 2006) could experience cloud-processing within a day.

Aqueous phase SO_2 oxidation in clouds is dominated by H_2O_2 oxidation (Seinfeld and Pandis, 1998; Liang and Jacobson, 1999; Warneck et al., 1999). The H_2O_2 oxidation reaction proceeds very fast and is independent of pH. The aqueous oxidation rate of SO_2 by H_2O_2 is $700\% \text{SO}_2 \text{h}^{-1} (\text{g water/m}^3)^{-1}$ at a H_2O_2 concentration of 1 ppb (Seinfeld and Pandis, 1998). In stratus and stratocumulus clouds, the typical water content is $\sim 0.3 \text{g/m}^3$ and a typical cloud-cycle is ~ 40 min (Seinfeld and Pandis, 1998; Feingold et al., 1998; Venkataraman et al., 2001). Such a cloud-cycle is estimated to

EC size distributions in an urban atmosphere in China

Xiao-Feng Huang and
Jian Zhen Yu

Title Page

Abstract

Introduction

Conclusions

References

Tables

Figures

⏪

⏩

◀

▶

Back

Close

Full Screen / Esc

Printer-friendly Version

Interactive Discussion

produce $55 \mu\text{g}/\text{m}^3 \text{SO}_4^{2-}$ at the assumed H_2O_2 and SO_2 concentrations in an open system scenario. The newly formed SO_4^{2-} adds onto the particles that have been activated to form liquid droplets. Upon cloud evaporation, residue particles of larger diameters are formed and the new particle diameters can be calculated from the sum of the original particle mass, sulfate ammonium newly acquired from the in-cloud processing, and absorbed water.

To estimate the particle growth, we first need to calculate the number of particles that are activated to form droplets prior to experiencing in-cloud processing. The saturation ratio (S) necessary for cloud activation of a particle with the diameter D_p is given by:

$$\ln S = \frac{A}{D_p} - \frac{B}{D_p^3 - d_u^3}, \quad (2)$$

where $A=4\sigma V_w/RT$, $B=6n_s V_w/\pi$, D_p is the whole particle diameter, d_u is the equivalent diameter of the insoluble material, σ is the surface tension, V_w is the molar volume of water, and n_s is the number of moles of solute in the particle. The maximum point of the Köhler curve resulting from Eq. (2) indicates the supersaturation necessary for activating particles of a certain size. Our calculation predicts that the critical supersaturation values (S_c) required to activate particles larger than 0.056, 0.1, 0.18, and $0.32 \mu\text{m}$ are 0.8%, 0.3%, 0.1%, and 0.04%, respectively. $S_c < 0.3\%$ is probably a realistic estimate. At this S_c value, the resulting activated CCN are in the order of several hundred per cm^3 , consistent with the order of magnitude of the droplet concentrations in low level clouds, such as stratus (Seinfeld and Pandis, 1998). Under the four S_c conditions, EC particles of $0.42 \mu\text{m}$ after cloud processing would grow to 0.52, 0.66, 0.86, and $1.2 \mu\text{m}$, respectively, in an open system scenario, which led to 140% gas-phase SO_2 converted to sulfate in a cloud cycle. In a closed system scenario, a cloud cycle could only transform a maximum of 100% of gas phase SO_2 , leading to growth of the original EC particles of $0.42 \mu\text{m}$ to $0.78 \mu\text{m}$ at $S_c=0.1\%$ and $1.1 \mu\text{m}$ at $S_c=0.04\%$.

Under lower S_c conditions, larger particles (and smaller in number) are activated to become cloud droplets. The newly produced ammonium sulfate is distributed among

EC size distributions in an urban atmosphere in China

Xiao-Feng Huang and
Jian Zhen Yu

[Title Page](#)[Abstract](#)[Introduction](#)[Conclusions](#)[References](#)[Tables](#)[Figures](#)[⏪](#)[⏩](#)[◀](#)[▶](#)[Back](#)[Close](#)[Full Screen / Esc](#)[Printer-friendly Version](#)[Interactive Discussion](#)

these larger particles to cause their growth. As a result, the lower S_c , the more prominent the growth of the particles in 0.32–0.56 μm size range. At the other extreme, at a high S_c value of 0.8%, all particles larger than 0.056 μm are activated to form cloud droplets. Due to the larger number of the smaller particles, less sulfate is available for the larger particles, leading to little growth of the larger particles.

Our calculation assuming either an open system or a closed system scenario indicates that in-cloud processing was a possible mechanism for the EC particles in the 0.32–0.56 μm size bin to grow to the 0.56–1.0 μm size bin in the atmosphere of Shenzhen. This conclusion is similar to the observation reported for sulfate aerosol in the 1987 Southern California Air Quality Study (SCAQS). Sulfate was observed to have two modes in the accumulation size range, with one peaking at 0.2 μm (the condensation mode) and the other one peaking at 0.7 μm (the droplet mode). Numerical analyses by Meng and Seinfeld (1994) and by Kerminen and Wexler (1995) demonstrated that in-cloud formation was the only possible mechanism for the growth of the condensation mode sulfate to the droplet mode sulfate. Although the prevalent meteorological conditions and aerosol chemical composition were different in the PRD region and in Southern California, it can be seen that in-cloud formation of sulfate is the only mechanism leading ambient aerosol particles $<0.5 \mu\text{m}$ grow to 0.7 μm or larger.

The above calculations were made using atmospheric conditions in the PRD region during the summer. It can be similarly argued that the EC modal peak in the 0.56–1.0 μm size bin observed in the winter samples could only be attributed to in-cloud processing of freshly emitted EC particles. In winter, gas-phase formation of H_2SO_4 would be slower because of lower temperature and less sunlight, and hence less effective in growing particles. In addition, lower cloud heights in winter would favor in-cloud processing, and thus more easily lead to the significant growth of EC.

3.3 Implications for the EC mixing state

The above analysis revealed that in-cloud processing was the only possible mechanism leading to growth of EC particles below 0.32–0.56 μm size bin to the next bigger size

EC size distributions in an urban atmosphere in China

Xiao-Feng Huang and
Jian Zhen Yu

Title Page

Abstract

Introduction

Conclusions

References

Tables

Figures

⏪

⏩

◀

▶

Back

Close

Full Screen / Esc

Printer-friendly Version

Interactive Discussion

bin. The residue particles after cloud-processing consist of internally mixed EC and $(\text{NH}_4)_2\text{SO}_4$. By assuming either all the EC is from vehicular emissions or other EC sources had similar EC size distribution patterns to EC from vehicular emissions, it is possible to estimate the fraction (R) of internally mixed EC particles due to cloud processing using Eq. (3):

$$R = (\alpha_a - \alpha_v) + (\alpha_a - \alpha_v) \times \frac{\alpha_v}{1 - \alpha_v}, \quad (3)$$
$$= (\alpha_a - \alpha_v) / (1 - \alpha_v)$$

where α_a and α_v are the mass fraction of EC in the 0.56–3.2 μm size range out of all EC mass in the accumulative size range (i.e. 0.056–3.2 μm) in ambient atmosphere and in vehicular emissions, respectively. $(1 - \alpha_v)$ is the mass fraction of EC in particles <0.56 μm freshly emitted from vehicles. The term $(\alpha_a - \alpha_v)$ is the percentage gain of EC mass in the droplet size range (i.e. 0.56–3.2 μm). This gain is mainly attributable to EC particles <0.56 μm growing into the size 0.56–3.2 μm through in-cloud processing. In a cloud event, when a portion of EC particles <0.56 μm grow into particles >0.56 μm , the larger EC particles (>0.56 μm) in the same air volume must also experience in-cloud processing and become internally mixed because the larger particles are more easily activated in cloud. The corresponding amount of larger particles that also experienced in-cloud processing was $(\alpha_a - \alpha_v) \times (\alpha_v / 1 - \alpha_v)$. The total internally mixed EC fraction (R) was therefore the sum of the two. R calculated this way is the lower limit estimate for the fraction of internally mixed EC, since other mechanisms (e.g., vapor condensation) can also lead to internal mixing of EC with sulfate but have not been considered in our estimation.

Using Eq. (3), we calculated the mass fraction of internally mixed EC in the accumulative size range to be 32% in the summer samples (22% for Group L samples and 39% for Group H samples) and 43% in the winter samples. In the droplet size range, the mass fraction of internally mixed EC was calculated to be 45% (Group L summer samples), 64% (Group H summer samples), and 68% (winter samples).

EC size distributions in an urban atmosphere in China

Xiao-Feng Huang and
Jian Zhen Yu

Title Page

Abstract

Introduction

Conclusions

References

Tables

Figures

⏪

⏩

◀

▶

Back

Close

Full Screen / Esc

Printer-friendly Version

Interactive Discussion

Cheng et al. (2006) recently studied the aerosol mixing state of EC at Xinken, a rural location in the PRD region in October 2004 using in situ aerosol microphysical and chemical measurements and a two-component aerosol optical model. They reported that internally mixed EC accounted for 5%~47% of the total EC mass under different meteorological conditions. Our estimate was in broad agreement with their estimates. That is, internally mixed EC accounts for a substantial fraction of the total EC in this region. Cheng et al. (2006) also observed that there was a fairly rapid local aging process transforming EC from external mixing to internal mixing. Our results showed that in-cloud processing could be the process that caused the rapid aging of EC.

4 Conclusions

We studied the size distribution characteristics of EC in the urban environment of the Pearl River Delta Region in China. The majority of EC (~80%) was found on fine particles less than $3.2\ \mu\text{m}$ in diameter. A consistent bimodal size distribution pattern was observed in the size range of $0.056\text{--}18\ \mu\text{m}$ in all samples. The fine mode peaked either at $0.42\ \mu\text{m}$ or $0.75\ \mu\text{m}$. The mode at $0.42\ \mu\text{m}$ could be ascribed to fresh vehicular emissions in this region, while the mode at $0.75\ \mu\text{m}$ was shown to be a result of in-cloud processing through theoretical investigation of all possible particle growth mechanisms. In-cloud processing leads to internally mixed EC and sulfate particles. Comparison of the EC size distributions in fresh vehicular emissions and in the ambient environment gave a lower end estimate of 45–60% of EC mass in the summer samples and 68% of EC mass in the winter samples in the droplet size range being internally mixed. Since the absorbance coefficients of particles of internally mixed EC and sulfate ammonium are much higher than in externally mixed EC, the fraction of internally mixed EC has to be considered in modeling atmospheric optical properties in this region. Our results also suggest that clouds indirectly modulate solar radiation by serving as the medium to mix EC and sulfate and thereby enhance the light absorbance capacities of aerosols.

EC size distributions in an urban atmosphere in China

Xiao-Feng Huang and
Jian Zhen Yu

Title Page

Abstract

Introduction

Conclusions

References

Tables

Figures

⏪

⏩

◀

▶

Back

Close

Full Screen / Esc

Printer-friendly Version

Interactive Discussion

Acknowledgements. The work was supported by the Research Grants Council of Hong Kong (605404 and 621405). We thank L.-Y. He at Peking University for support during sampling.

References

Birch, M. E. and Cary, R. A.: Black carbon-based method for monitoring occupational exposures to particulate diesel exhaust, *Aerosol Sci. Technol.*, 25, 221–241, 1996.

Cao, J. J., Lee, S. C., Ho, K. F., Zou, S. C., Fung, K., Li, Y., Watson, J. G., and Chow, J. C.: Spatial and seasonal variations of atmospheric organic carbon and elemental carbon in Pearl River Delta Region, China, *Atmos. Environ.*, 38, 4447–4456, 2004.

Cheng, Y. F., Eichler, H., Wiedensohler, A., et al.: Mixing state of elemental carbon and non-light-absorbing aerosol components derived from in situ particle optical properties at Xinken in Pearl River Delta of China, *J. Geophys. Res.*, 111, D20204, doi:10.1029/2005JD006929, 2006.

Chow, J. C., Watson, J. G., and Pritchett, L. C.: The DRI thermal/optical reflectance carbon analysis system: description, evaluation and applications in U.S. air quality studies, *Atmos. Environ.*, 27A, 1185–1201, 1993.

Chuang, P. Y., Duvall, R. M., Bae, M. S., Jefferson, A., Schauer, J. J., Yang, H., Yu, J. Z., and Kim, J.: Observations of elemental carbon and absorption during ACE-Asia and implications for aerosol radiative properties and climate forcing, *J. Geophys. Res.*, 108(D23), 8634, doi:10.1029/2002JD003254, 2003.

Ervens, B., George, C., Williams, J. E., Buxton, G. V., Salmon, G. A., Bydder, M., Wilkinson, F., Dentener, F., Mirabel, P., Wolke, R., and Herrmann, H.: CAPRAM 2.4 (MODAC mechanism): An extended and condensed tropospheric aqueous phase mechanism and its application, *J. Geophys. Res.*, 108(D14), 4426, doi:10.1029/2002JD002202, 2003.

Feingold, G., Kreidenweis, S. M., and Zhang, Y.: Stratocumulus processing of gases and cloud condensation nuclei. 1. Trajectory ensemble model, *J. Geophys. Res.*, 103, 19 527–19 542, 1998.

Hagler, G. S. W., Bergin, M. H., Salmon, L. G., Yu, J. Z., Wan, E. C. H., Zheng, M., Zeng, L. M., Zhang, Y. H., Lau, A. K. H., and Schauer, J. J.: Source areas and chemical composition of fine particulate matter in the Pearl River Delta region of China, *Atmos. Environ.*, 40, 3802–3815, 2006.

Hansen, J., Sato, M., Ruedy, R., Lacis, A., and Oinas, V.: Global warming in the twenty-first century: an alternative scenario, *Proc. Natl. Academy Sci.*, 97, 9875–9880, 2000.

ACPD

7, 10743–10766, 2007

EC size distributions in an urban atmosphere in China

Xiao-Feng Huang and
Jian Zhen Yu

Title Page

Abstract

Introduction

Conclusions

References

Tables

Figures

◀

▶

◀

▶

Back

Close

Full Screen / Esc

Printer-friendly Version

Interactive Discussion

- Haywood, J. M. and Shine, K. P.: The effect of anthropogenic sulphate and soot aerosol on the clear sky planetary radiation budget, *Geophys. Res. Lett.*, 22, 603–606, 1995.
- Horvath, H.: Atmospheric light absorption—a review, *Atmos. Environ.*, 27A, 293–317, 1993.
- Huang, X. F., Yu, J. Z., He, L. Y., and Hu, M.: Size distribution characteristics of elemental carbon emitted from Chinese vehicles: Results of a tunnel study and atmospheric implications, *Environ. Sci. Technol.*, 44, 5355–5360, 2006a.
- Huang, X.-F., Yu, J. Z., He, L.-Y., and Yuan, Z.: Water-soluble organic carbon and oxalate in aerosols at a coastal urban site in China: Size distribution characteristics, sources, and formation mechanisms, *J. Geophys. Res.*, 111, D22212, doi:10.1029/2006JD007408, 2006b.
- Jacobson, M. Z.: A physically-based treatment of elemental carbon optics: Implications for global direct forcing of aerosols, *Geophys. Res. Lett.*, 27, 217–220, 2000.
- Jacobson, M. Z.: Strong radiative heating due to the mixing state of black carbon in atmospheric aerosols, *Nature*, 409, 695–697, 2001.
- Kerminen, V.-M. and Wexler, A. S.: Growth laws for atmospheric aerosol particles: An examination of the bimodality of the accumulation mode, *Atmos. Environ.*, 29, 3263–3275, 1995.
- Kerminen, V.-M., Pirjola, L., Boy, M., et al.: Interaction between SO₂ and submicron atmospheric particles, *Atmos. Res.*, 54, 41–57, 2000.
- Langner, J. and Rodhe, H.: A global 3-dimensional model of the tropospheric sulfur cycle, *J. Atmos. Chem.*, 13, 225–263, 1991.
- Lesins, G., Chylek, P., and Lohmann, U.: A study of internal and external mixing scenarios and its effect on aerosol optical properties and direct radiative forcing, *J. Geophys. Res.*, 107(D10), 4094, doi:10.1029/2001JD000973, 2002.
- Liang, J. and Jacobson, M. Z.: A study of sulfur dioxide oxidation pathways over a range of liquid water contents, pH values, and temperatures, *J. Geophys. Res.*, 104, 13 749–13 769, 1999.
- Louie, P. K. K., Watson, J. G., Chow, J. C., Chen, L. W. A., Sin, D. W. M., and Lau, A. K. H.: Seasonal characteristics and regional transport of PM_{2.5} in Hong Kong, *Atmos. Environ.*, 39, 1695–1710, 2005.
- McHenry, J. N. and Dennis, R. L.: The relative importance of oxidation pathways and clouds to atmospheric ambient sulfate production as predicted by the regional acid deposition model, *J. Appl. Meteorol.*, 33, 890–905, 1994.
- Meng, Z. and Seinfeld, J. H.: On the source of the submicrometer droplet mode of urban and regional aerosols, *Aerosol Sci. Technol.*, 20, 253–265, 1994.

**EC size distributions
in an urban
atmosphere in China**

Xiao-Feng Huang and
Jian Zhen Yu

[Title Page](#)[Abstract](#)[Introduction](#)[Conclusions](#)[References](#)[Tables](#)[Figures](#)[⏪](#)[⏩](#)[◀](#)[▶](#)[Back](#)[Close](#)[Full Screen / Esc](#)[Printer-friendly Version](#)[Interactive Discussion](#)

- Menon, S., Hansen, J., Nazarenko, L., and Luo, Y.: Climate effects of black carbon aerosols in China and India, *Science*, 297, 2250–2253, 2002.
- Nenes, A., Pilinis, C., and Pandis, S. N.: Continued development and testing of a new thermodynamic aerosol module for urban and regional air quality models, *Atmos. Environ.*, 33, 1553–1560, 1998.
- 5 NIOSH: Method 5040 Issue 3: Elemental carbon (diesel exhaust). In NIOSH manual of analytical methods, 4th ed., National Institute of Occupational Safety and Health, Cincinnati, 1999.
- Pandis, S. N., Wexler, A. S., and Seinfeld, J. H.: Secondary organic aerosol formation and transport. 2. Predicting the ambient secondary organic aerosol-size distribution, *Atmos. Environ.*, 27A, 2403–2416, 1993.
- 10 Saxena, P. and Seigneur, C.: On the oxidation of SO₂ to sulfate in atmospheric aerosols, *Atmos. Environ.*, 21, 807–812, 1987.
- Seinfeld, J. H. and Pandis, S. N.: Atmospheric chemistry and physics: from air pollution to climate change, John Wiley, New York, 1998.
- 15 Shenzhen Environmental Protection Bureau (SZEPPB): Environmental monitoring report of Shenzhen, 2005, Shenzhen, China, 2006.
- Venkataraman, C., Mehra, A., and Mhaskar, P.: Mechanisms of sulphate aerosol production in clouds: effect of cloud characteristics and season in the Indian region, *Tellus*, 53B, 260–272, 2001.
- 20 Warneck, P.: The relative importance of various pathways for the oxidation of sulphur dioxide and nitrogen dioxide in sunlit continental fair weather clouds, *Phys. Chem. Chem. Phys.*, 1, 5471–5483, 1999.
- Wexler, A. S., Lurmann, F. W., and Seinfeld, J. H.: Modelling urban and regional aerosols—I. Model development, *Atmos. Environ.*, 28, 531–546, 1994.
- 25 Yu, J. Z., Tung, J. W. T., Wu, A. W. M., Lau, A. K. H., Louie, P. K. K., and Fung, J. C. H.: Abundance and seasonal characteristics of elemental and organic carbon in Hong Kong PM₁₀, *Atmos. Environ.*, 38, 1511–1521, 2004.
- Yuan, Z. B., Yu, J. Z., Lau, A. K. H., Louie, P. K. K., and Fung, J. C. H.: Application of positive matrix factorization in estimating aerosol secondary organic carbon in Hong Kong and its relationship with secondary sulfate, *Atmos. Chem. Phys.*, 6, 25–34, 2006,
<http://www.atmos-chem-phys.net/6/25/2006/>.

**EC size distributions
in an urban
atmosphere in China**

Xiao-Feng Huang and
Jian Zhen Yu

[Title Page](#)[Abstract](#)[Introduction](#)[Conclusions](#)[References](#)[Tables](#)[Figures](#)[⏪](#)[⏩](#)[◀](#)[▶](#)[Back](#)[Close](#)[Full Screen / Esc](#)[Printer-friendly Version](#)[Interactive Discussion](#)

EC size distributions in an urban atmosphere in China

Xiao-Feng Huang and
Jian Zhen Yu

Title Page

Abstract

Introduction

Conclusions

References

Tables

Figures

⏪

⏩

◀

▶

Back

Close

Full Screen / Esc

Printer-friendly Version

Interactive Discussion

Table 1. EC concentrations in fine and coarse particles in Shenzhen ($\mu\text{g}/\text{m}^3$)*.

Sample #	Sampling period	fine	coarse	Sample #	Sampling period	fine	coarse
S1	21–22 July 2004	2.7	0.90	W1	14–15 Dec 2004	18.4	4.5
S2	23–24 July 2004	3.5	1.1	W2	16–17 Dec 2004	13.1	2.8
S3	25–26 July 2004	2.3	0.72	W3	18–19 Dec 2004	15.4	3.3
S4	12–13 Aug 2004	7.2	1.4	W4	20–21 Dec 2004	7.2	1.1
S5	14–16 Aug 2004	2.7	0.91	W5	22–23 Dec 2004	6.8	1.8
S6	17–18 Aug 2004	11.4	2.5	W6	24–25 Dec 2004	6.1	1.1
S7	21–23 Aug 2004	4.2	1.0	W7	26–27 Dec 2004	4.1	0.93
S8	24–26 Aug 2004	4.7	1.1	W8	28–29 Dec 2004	3.8	0.53
S9	1–3 Sep 2004	2.2	0.61	W9	30–31 Dec 2004	3.3	0.67
				W10	1–2 Jan 2005	3.9	0.81
				W11	3–4 Jan 2005	7.7	1.5
				W12	5–6 Jan 2005	7.3	0.80
AVE		4.5	1.1			8.1	1.6
SD		3.0	0.58			4.9	1.2

* The EC concentrations might be overestimated because no charring correction was considered in the thermal analysis.

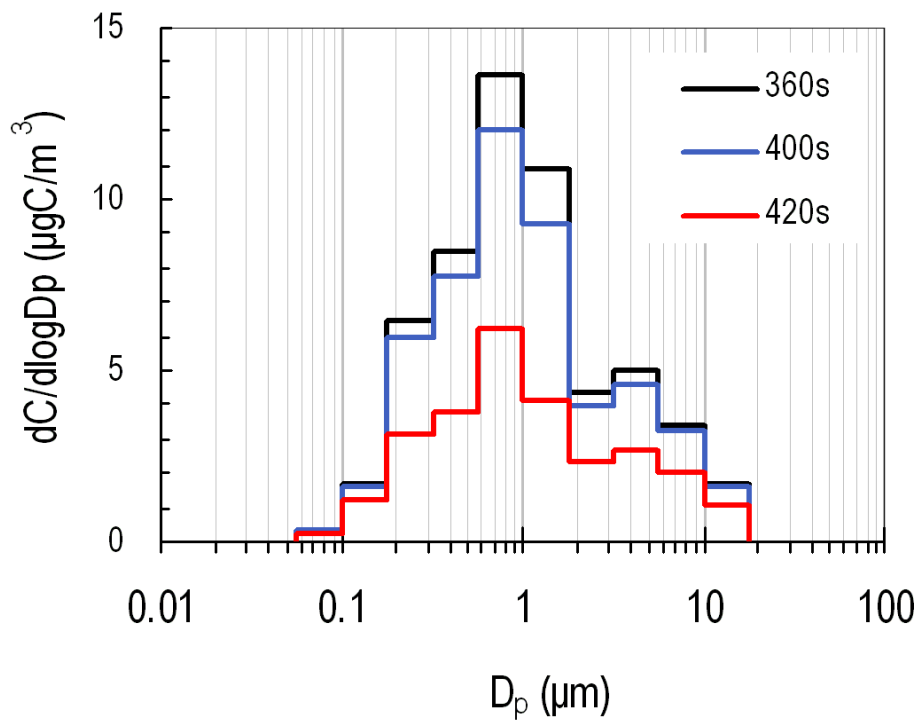
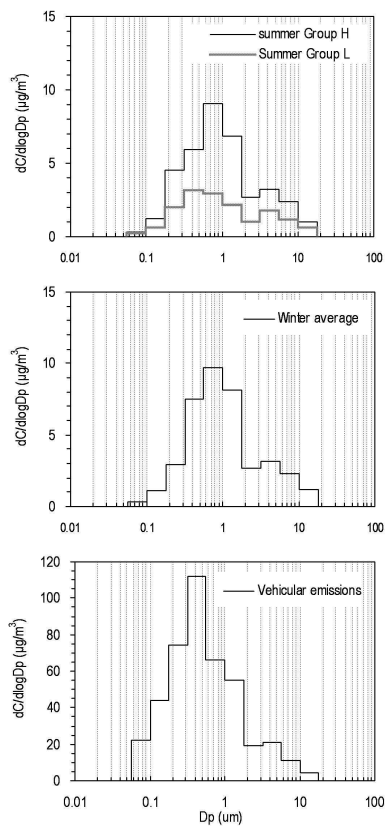
**EC size distributions
in an urban
atmosphere in China**Xiao-Feng Huang and
Jian Zhen Yu

Fig. 1. Comparison of EC size distributions using different OC/EC split times.

[Title Page](#)[Abstract](#)[Introduction](#)[Conclusions](#)[References](#)[Tables](#)[Figures](#)[◀](#)[▶](#)[◀](#)[▶](#)[Back](#)[Close](#)[Full Screen / Esc](#)[Printer-friendly Version](#)[Interactive Discussion](#)

**EC size distributions
in an urban
atmosphere in China**Xiao-Feng Huang and
Jian Zhen Yu**Fig. 2.** Average EC size distributions in ambient samples and in vehicular emissions.[Title Page](#)[Abstract](#)[Introduction](#)[Conclusions](#)[References](#)[Tables](#)[Figures](#)[◀](#)[▶](#)[◀](#)[▶](#)[Back](#)[Close](#)[Full Screen / Esc](#)[Printer-friendly Version](#)[Interactive Discussion](#)

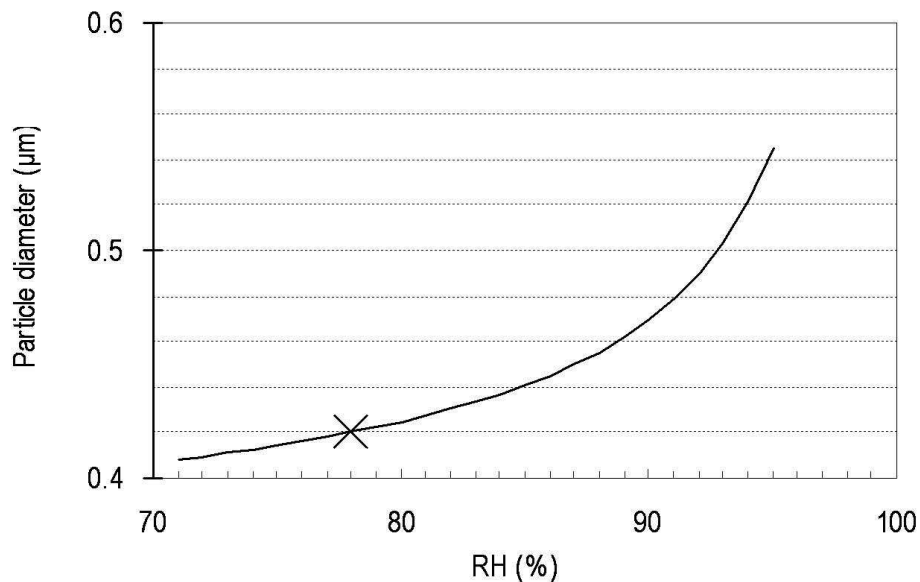
**EC size distributions
in an urban
atmosphere in China**Xiao-Feng Huang and
Jian Zhen Yu

Fig. 3. Hygroscopic growth of particles at $0.42\ \mu\text{m}$ in summer (the cross corresponding to $0.42\ \mu\text{m}$ at RH 78%, the mean RH value during the summer sampling periods).

[Title Page](#)[Abstract](#)[Introduction](#)[Conclusions](#)[References](#)[Tables](#)[Figures](#)[⏪](#)[⏩](#)[◀](#)[▶](#)[Back](#)[Close](#)[Full Screen / Esc](#)[Printer-friendly Version](#)[Interactive Discussion](#)

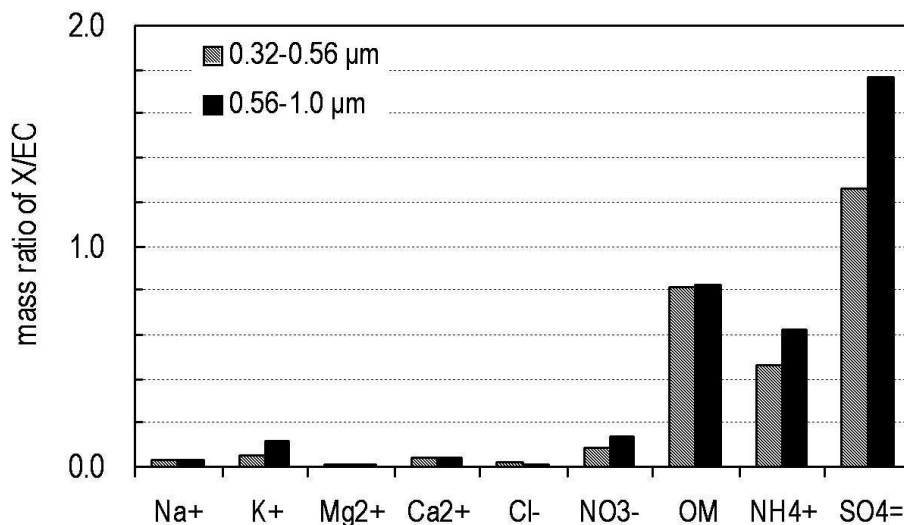
**EC size distributions
in an urban
atmosphere in China**Xiao-Feng Huang and
Jian Zhen Yu

Fig. 4. Comparison of abundances of major constituents relative to EC in the size bins of 0.32–0.56 μm and 0.56–1.0 μm in Group H samples.

[Title Page](#)[Abstract](#)[Introduction](#)[Conclusions](#)[References](#)[Tables](#)[Figures](#)[⏪](#)[⏩](#)[◀](#)[▶](#)[Back](#)[Close](#)[Full Screen / Esc](#)[Printer-friendly Version](#)[Interactive Discussion](#)

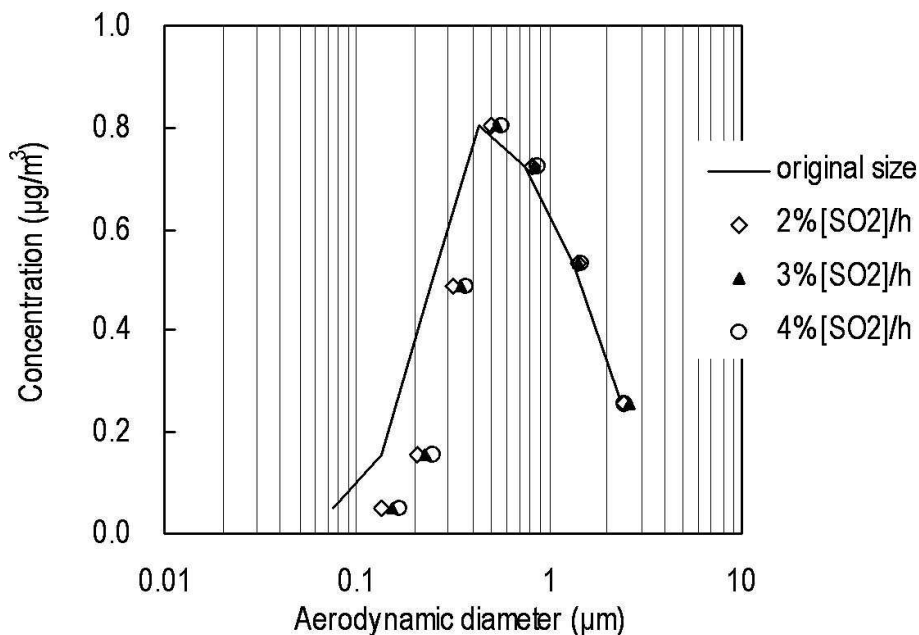
**EC size distributions
in an urban
atmosphere in China**Xiao-Feng Huang and
Jian Zhen Yu

Fig. 5. Particle growth through H_2SO_4 vapor condensation. Three H_2SO_4 formation rates, 2%, 3%, and 4% $[\text{SO}_2]/\text{h}$, were assumed corresponding to $[\text{OH}]$ concentration of 0.5, 0.75, and 1.0×10^7 molecules cm^{-3} .

[Title Page](#)[Abstract](#)[Introduction](#)[Conclusions](#)[References](#)[Tables](#)[Figures](#)[◀](#)[▶](#)[◀](#)[▶](#)[Back](#)[Close](#)[Full Screen / Esc](#)[Printer-friendly Version](#)[Interactive Discussion](#)